V. K. Ignatovich [1], V. V. Nesvizhevsky [2]

REFLECTION OF SLOW NEUTRONS
FROM POWDER OF NANORODS

[1] E-mail: v.ignatovi@gmail.com
[2] Institut Max von Laue – Paul Langevin, Grenoble, France;
e-mail: nesvizhevsky@ill.eu

Игнатович В. К., Несвижевский В. В.   E4-2013-106

Отражение медленных нейтронов от порошка наностержней

Недавно обнаружено явление эффективного диффузного отражения очень холодных нейтронов (ОХН) от наноструктурированного вещества при любом угле их падения на его поверхность, а также квазизеркальное отражение холодных нейтронов (ХН) от наноструктурированного вещества при их падении на его поверхность под малыми углами. В обоих случаях в качестве наноструктурированного вещества использовался порошок алмазных наночастиц, а измеренные вероятности отражения намного превышали характеристики известных альтернативных отражателей. Оба эти явления уже нашли применение в нейтронном эксперименте и при создании нейтронных источников. В настоящей теоретической работе рассматривается возможность дополнительного увеличения эффективности наноструктурированных отражателей при замене сферических наночастиц наностержнями. Показано, что альбедо ОХН от порошка разупорядоченных наностержней ниже, чем их альбедо от порошка наносфер того же диаметра. Однако альбедо ОХН и квазизеркальное отражение ХН от порошка длинных наностержней, ориентированных параллельно его поверхности, превышает соответствующие значения для отражателя из наносфер того же диаметра.

Ignatovich V. K., Nesvizhevsky V. V.   E4-2013-106

Reflection of Slow Neutrons from Powder of Nanorods

Two phenomena were recently observed: efficient diffuse reflection of very cold neutrons (VCN) from nanostructured matter for any angle of neutron incidence to the matter surface, and also quasispecular reflection of cold neutrons (CN) from nanostructured matter for small angles of neutron incidence to the matter surface. In both cases, powder of diamond nanoparticles was used as nanostructured matter, and the measured reflection probabilities by far exceeded the values known for alternative reflectors. Both these phenomena are already used in neutron experiments and for building neutron sources. In the present theoretical work, we consider an option of further increasing the efficiency of nanostructured reflectors due to replacing spherical nanoparticles by nanorods. We showed that VCN albedo from powder of randomly oriented nanorods is lower than their albedo from powder of nanospheres of equal diameter. However, albedo of VCN and quasispecular reflection of CN from powder of long nanorods oriented parallel to the powder surface exceed those for powder of nanospheres of equal diameter.

1. INTRODUCTION

Efficient neutron reflectors are needed in experiments as well as for building neutron sources. For ultracold neutrons (UCN) [1–3] ($< 10^{-7}$ eV), neutron optical potential of matter is nearly the ideal reflector, which provides the probability of elastic reflection close to unit, at any temperature of matter. For neutrons with the energy of up to $10^{-6(5)}$ eV, one uses multi-layer coatings (supermirrors) [4–5], which provide the probability of specular elastic reflection of up to 80–90 %. Until recently, efficient reflectors of neutrons with the energy of up to $10^{-2(3)}$ eV had not been known. At the energy of $\sim 10^{-2}$ eV, neutron wavelength is comparable with interatomic distances thus effects of elastic diffraction and diffuse reflection in respectively ordered and disordered matter appear. At even larger energies, inelastic processes, which provide moderation and reflection of neutrons in nuclear reactors [6], prevail.

Two phenomena were observed recently: efficient diffuse reflection of very cold neutrons (VCN) from nanostructured matter for any angle of neutron incidence to the matter surface, and also quasi-specular reflection of cold neutrons (CN) from nano-structured matter for small angles of neutron incidence to the matter surface [7–14]. In both cases, powder of diamond nanoparticles was used as nano-structured matter, and the measured reflection probabilities by far exceeded the values for known alternative reflectors. Both these phenomena are already used in neutron experiments and for building neutron sources. In the present theoretical work, we consider an option of further increasing the efficiency of nanostructured reflectors due to replacing spherical nanoparticles by nanorods. For concreteness, we choose two values of neutron velocity: 1) 50 m/s, as nanostructured reflectors are very efficient at this neutron velocity, and 2) 450 m/s, as, on the one hand, the efficiency of nanostructured reflectors made of nanospheres rapidly decreases at this neutron velocity and, on the other hand, such reflectors are highly requested, for instance, for increasing UCN density in UCN sources based on superfluid helium [15, 16], used in particular for the GRANIT spectrometer [17], aiming at studies of/with quantum states of neutrons in gravitational and centrifugal potentials [18, 19, 29–31].

If optical potential of a nanorod material is much smaller than neutron kinetic energy and if neutron scattering cross section is much smaller than geometrical

cross section of the nanorod, then the amplitude of neutron scattering can be calculated using perturbation theory. These approximations are valid for all cases of interest in the present work. In this case, the amplitude $F(\mathbf{q}, \mathbf{l})$ of neutron scattering at a nanorod with a radius ρ and a length $2a$ with an axis along the unit vector $\mathbf{l}$ equals:

$$
\begin{aligned}
F(\mathbf{q}, \mathbf{l}) &= N_0 b \int_{V_1} d^3 r \, \exp\left(i\mathbf{q} \cdot \mathbf{r}\right) = \\
&= N_0 b \int_{-a}^{a} dz_l \int_0^{\rho} \rho' d\rho' \int_0^{2\pi} d\varphi \, \exp\left(iq_l z_l + iq_\rho \rho' \cos\varphi\right) = \\
&= \frac{4\pi N_0 b}{q_l} \sin\left(q_l a\right) \int_0^{\rho} \rho' d\rho' J_0(q_\rho \rho') = u_0 a \rho^2 \, \mathrm{sinc}\left(q_l a\right) \frac{J_1(q_\rho \rho)}{q_\rho \rho}, \quad (1)
\end{aligned}
$$

where $\mathrm{sinc}\,(x) = \sin(x)/x$, $u_0 = 4\pi N_0 b$ is the potential of neutron interaction with the nanorod matter divided by a factor $\hbar^2/2m$ (m is the neutron mass, $\hbar$ is the reduced Planck constant); N_0 is the number of atoms in the unit volume of the nanorod; b is the length of neutron coherent scattering on a nucleus of the nanorod matter; $\mathbf{q} = \mathbf{k}_0 - k$ is the transferred momentum; $\mathbf{k}_0$, $\mathbf{k}$ are momenta of the neutron before and after scattering; $q_l = \mathbf{q} \cdot \mathbf{l}$; $q_\rho = \sqrt{\mathbf{q}^2 - (\mathbf{q} \cdot \mathbf{l})^2}$, $J_0(x)$ and $J_1(\mathrm{x})$ are Bessel functions; and we also used the following expressions: $J_0(x) = \int_0^{2\pi} \frac{d\varphi}{2\pi} \exp\left(ix \cos\varphi\right)$, and $\int_0^x x' dx' J_0(x') = x J_1(x)$.

In this work, we consider neutron scattering on diamond nanorods. The potential of interaction of a neutron with a nanorod matter is always assumed to be equal to 300 neV, as it is for neutron scattering at crystal diamond. This approximation is valid in the first order for nanospheres [22] as well as for nanorods [20], because their densities are close to the density of bulk diamond, and their shells are not very thick [21, 23, 24]. However, more accurate but also more bulky descriptions will be required for concrete reflector realizations.

The refection is understood here as albedo, i.e., the probability of neutron reflection integrated over all backward angles. We will calculate albedo following works [25–27], and will remind below briefly the calculation method.

2. METHOD OF ALBEDO CALCULATION

First, we will define notations. A neutron moving along a solid angle Ω with the polar axis along the internal normal to the matter surface is defined by the state vector $|\Omega\rangle$. An angular distribution $P(\Omega)$ will be characterized by the state vector

$$
|P\rangle = \int_{4\pi} P(\Omega) d\Omega |\Omega\rangle. \tag{2}
$$

2

The norm of this state $N_P = \int_{4\pi} P(\Omega)\,d\Omega$ is calculated by means of multiplication of Eq. (2) from the left by a meter $|m\rangle = \int_{4\pi} d\Omega|\Omega\rangle$, using a natural relation $\langle\Omega||\Omega'\rangle = \delta(\Omega - \Omega')$. In particular, isotropic distribution of incident and reflected neutrons corresponds to the state

$$|P_{is}\rangle = \int_{2\pi} \frac{|\cos\theta|}{\pi}\,d\Omega|\Omega\rangle. \tag{3}$$

Its norm is unit.

A scatterer, which transforms a neutron state $|\Omega'\rangle$ to a state $|\Omega\rangle$ with a probability $w(\Omega \leftarrow \Omega')$, is described by means of an operator $\hat{\mathbf{W}} = \int_{4\pi} |\Omega\rangle w(\Omega \leftarrow \Omega')\langle\Omega'|\,d\Omega d\Omega'$. A neutron from a state (2) is scattered into the state

$$|P'\rangle = \hat{\mathbf{W}}|P\rangle = \int_{4\pi} |\Omega\rangle w(\Omega \leftarrow \Omega')P(\Omega')d\Omega d\Omega' = \int_{4\pi} P'(\Omega)|\Omega\rangle\,d\Omega, \tag{4}$$

where $P'(\Omega) = \int_{4\pi} w(\Omega \leftarrow \Omega')P(\Omega')\,d\Omega'$.

In order to calculate albedo R_D from a layer of powder with a finite thickness D, one first calculates albedo R_∞ from an infinitely thick layer. For this purpose, one splits a layer of small thickness ξ from the infinite one; scattering on this layer is calculated using perturbation theory, and it is presented in a form of a reflection $\hat{\rho}_\xi$ and a transmission $\hat{\tau}_\xi$ operators. In order to find the operator $\hat{\mathbf{R}}_\infty$ of reflection from an infinitely thick layer for incident neutrons in a state $|\Omega_0\rangle$, one has to know their distribution $|X_\xi\rangle = \hat{\mathbf{X}}_\xi|\Omega_0\rangle$ behind the thin layer. For the operator $\hat{\mathbf{X}}_\xi$, one could write a self-consistent equation

$$\hat{\mathbf{X}}_\xi = \hat{\tau}_\xi + \hat{\rho}_\xi\hat{\mathbf{R}}_\infty\hat{\mathbf{X}}_\xi, \tag{5}$$

which shows that $\hat{\mathbf{X}}_\xi$ is constructed from the transmission through the layer ξ and from the contribution $\hat{\mathbf{X}}_\xi$ itself, as a neutron behind the layer ξ is reflected from the infinite layer then is reflected ones again from the layer ξ, then is returned to the infinitely thick layer, where the state $|X_\xi\rangle$ is formed together with the part characterized by the transmission $\hat{\tau}_\xi$.

If we know $\hat{\mathbf{X}}_\xi$, we can write an equation for $\hat{\mathbf{R}}_\infty$:

$$\hat{\mathbf{R}}_\infty = \hat{\rho}_\xi + \hat{\tau}_\xi\hat{\mathbf{R}}_\infty\hat{\mathbf{X}}_\xi. \tag{6}$$

After expressing $\hat{\mathbf{X}}_\xi$ via Eq. (5):

$$\hat{\mathbf{X}}_\xi = \left(\hat{\mathbf{I}} - \hat{\rho}_\xi\hat{\mathbf{R}}_\infty\right)^{-1}\hat{\tau}_\xi, \tag{7}$$

where $\hat{\mathbf{I}} = \int_{4\pi} |\Omega\rangle\,d\Omega\langle\Omega|$ is the unit operator, and substituting the result into Eq. (6), one gets

$$\hat{\mathbf{R}}_\infty = \hat{\rho}_\xi + \hat{\tau}_\xi\hat{\mathbf{R}}_\infty\left(1 - \hat{\rho}_\xi\hat{\mathbf{R}}_\infty\right)^{-1}\hat{\tau}_\xi. \tag{8}$$

3

Operators $\hat{\boldsymbol{\rho}}_\xi$ and $\hat{\boldsymbol{\tau}}_\xi$ are related to macroscopic scattering cross sections as

$$\hat{\boldsymbol{\rho}}_\xi = \xi\hat{\boldsymbol{\Sigma}}_b, \quad \hat{\boldsymbol{\tau}}_\xi = \hat{\mathbf{I}} + \xi\hat{\boldsymbol{\Sigma}}_f - \xi\Sigma_t\hat{\mathbf{S}}, \tag{9}$$

where

$$\hat{\boldsymbol{\Sigma}}_b = \int_{\mathbf{n}\boldsymbol{\Omega}<0} d\Omega \int_{\mathbf{n}\boldsymbol{\Omega}'>0} |\Omega\rangle \Sigma_s(\Omega \leftarrow \Omega')\frac{d\Omega'}{\cos\theta'}\langle\Omega'| =$$
$$= \int_{\mathbf{n}\boldsymbol{\Omega}>0} d\Omega \int_{\mathbf{n}\boldsymbol{\Omega}'<0} |\Omega\rangle \Sigma_s(\Omega \leftarrow \Omega')\frac{d\Omega'}{\cos\theta'}\langle\Omega'| \tag{10}$$

is the operator of back scattering from the left or from the right,

$$\hat{\boldsymbol{\Sigma}}_f = \int_{\mathbf{n}\boldsymbol{\Omega}>0} d\Omega \int_{\mathbf{n}\boldsymbol{\Omega}'>0} |\Omega\rangle \Sigma_s(\Omega \leftarrow \Omega')\frac{d\Omega'}{\cos\theta'}\langle\Omega'| =$$
$$= \int_{\mathbf{n}\boldsymbol{\Omega}<0} d\Omega \int_{\mathbf{n}\boldsymbol{\Omega}'<0} |\Omega\rangle \Sigma_s(\Omega \leftarrow \Omega')\frac{d\Omega'}{\cos\theta'}\langle\Omega'| \tag{11}$$

is the operator of forward scattering from the left or right; $\Sigma_s(\Omega \leftarrow \Omega')$ is the differential macroscopic scattering cross section; $\Sigma_t = \Sigma_s + \Sigma_a$ is the total macroscopic cross section, consisting of the integral scattering Σ_s and absorption Σ_a cross sections; and

$$\hat{\mathbf{S}} = \int_{2\pi} |\Omega'\rangle\frac{d\Omega'}{\cos\theta'}\langle\Omega'| \tag{12}$$

is an operator, which takes into account that the number of scatterers along the neutron path increases with increasing of the incidence angle.

At small value of ξ Eq. (8) can be linearized and reduced to the form

$$\hat{\mathbf{R}}_\infty\hat{\boldsymbol{\Sigma}}_b\hat{\mathbf{R}}_\infty + \left(\hat{\boldsymbol{\Sigma}}_f - \Sigma_t\hat{\mathbf{S}}\right)\hat{\mathbf{R}}_\infty + \hat{\mathbf{R}}_\infty\left(\hat{\boldsymbol{\Sigma}}_f - \Sigma_t\hat{\mathbf{S}}\right) + \hat{\boldsymbol{\Sigma}}_b = 0. \tag{13}$$

We suppose that the distribution of reflected neutrons is isotropic, and represent the solution of (13) in the form

$$\hat{\mathbf{R}}_\infty = R_\infty \int_{\mathbf{n}\boldsymbol{\Omega}<0} |\Omega\rangle\frac{|\cos\theta|}{\pi}d\Omega \int_{\mathbf{n}\boldsymbol{\Omega}>0} d\Omega'\langle\Omega'| = R_\infty|P_{is}\rangle\langle m|. \tag{14}$$

Substitute it in (13) and multiply (13) from the left by $\langle m|$ and from the right by $|P_{is}\rangle$. Then we will get

$$R_\infty^2\Sigma_b + 2R_\infty\left(\Sigma_f - \Sigma_t\right) + \Sigma_b = 0, \tag{15}$$

4

where

$$\Sigma_b = \int_{\mathbf{n\Omega}<0} d\Omega \int_{\mathbf{n\Omega'}>0} \Sigma_s(\Omega \leftarrow \Omega')\frac{d\Omega'}{2\pi} =$$
$$= \int_{\mathbf{n\Omega}>0} d\Omega \int_{\mathbf{n\Omega'}<0} \Sigma_s(\Omega \leftarrow \Omega')\frac{d\Omega'}{2\pi}, \quad (16)$$

$$\Sigma_f = \int_{\mathbf{n\Omega}<0} d\Omega \int_{\mathbf{n\Omega'}<0} \Sigma_s(\Omega \leftarrow \Omega')\frac{d\Omega'}{2\pi} =$$
$$= \int_{\mathbf{n\Omega}>0} d\Omega \int_{\mathbf{n\Omega'}>0} \Sigma_s(\Omega \leftarrow \Omega')\frac{d\Omega'}{2\pi} \quad (17)$$

are macroscopic cross sections of backward and forward scattering. Since $\Sigma_s = \Sigma_t + \Sigma_b$, then $\Sigma_t = \Sigma_s + \Sigma_a = \Sigma_t + \Sigma_b + \Sigma_a$, and the solution of Eq. (5) can be presented in the form

$$R_\infty = \frac{\sqrt{2\Sigma_b + \Sigma_a} - \sqrt{\Sigma_a}}{\sqrt{2\Sigma_b + \Sigma_a} + \sqrt{\Sigma_a}} = \frac{\sqrt{1 + 2\Sigma_b/\Sigma_a} - 1}{\sqrt{1 + 2\Sigma_b/\Sigma_a} + 1}. \quad (18)$$

In order to calculate albedo from a wall of a finite thickness, one has to know a law of attenuation of neutron intensity in the matter. It follows from Eq. (7). After linearization of this expression at small ξ, and substitution of Eq. (14) into it, as well as multiplication from left by $\langle m|$, and from right by $|P_{is}\rangle$, one gets $\langle m|\hat{\mathbf{X}}_\xi|P_{is}\rangle \approx \exp(-\xi/L)$, where

$$1/L = 2\sqrt{2\Sigma_b + \Sigma_a}\sqrt{\Sigma_a} = 2\Sigma_a\sqrt{1 + 2\Sigma_b/\Sigma_a}. \quad (19)$$

Thus $\hat{\mathbf{X}}_z$ at a depth z can be presented in the form

$$\hat{\mathbf{X}}_z = |P_{is}\rangle \exp(-z/L)\langle m|. \quad (20)$$

For calculating reflection $\hat{\mathbf{R}}_D$ and transmission $\hat{\mathbf{T}}_D$ from/through a layer with a thickness D, we will use Eqs. (5) and (6) splitting a layer of a finite thickness D from the infinite one.
The equations will look:

$$\hat{\mathbf{X}}_D = \hat{\mathbf{T}}_D + \hat{\mathbf{R}}_D\hat{\mathbf{R}}_\infty\hat{\mathbf{X}}_D, \quad \hat{\mathbf{R}}_\infty = \hat{\mathbf{R}}_D + \hat{\mathbf{T}}_D\hat{\mathbf{R}}_\infty\hat{\mathbf{X}}_D, \quad (21)$$

and they can be resolved with respect to $\hat{\mathbf{R}}_D$ and $\hat{\mathbf{T}}_D$ for known $\hat{\mathbf{R}}_\infty$ and $\hat{\mathbf{X}}_D$. Assuming $\hat{\mathbf{R}}_D$ to be isotropic, we get

$$R_D = R_\infty \frac{1 - \exp(-2D/L)}{1 - R_\infty^2 \exp(-2D/L)}. \quad (22)$$

5

It follows from Eqs. (18) and (19) that in order to calculate R_D, which will be named below as simply R, one has to get macroscopic cross sections Σ_a and Σ_b, overaged over angles, however for that, one has to know differential cross sections.

3. CALCULATION OF MACROSCOPIC CROSS SECTIONS

From the scattering amplitude (1), one could calculate the differential cross section

$$d\sigma(\mathbf{q}, \mathbf{l})/d\Omega = |F(\mathbf{q}, \mathbf{l})|^2 = u_0^2 a^2 \rho^4 \sin c^2(\mathbf{q}\mathbf{l}a) \left| \frac{J_i(q_\rho \rho)}{q_\rho \rho} \right|^2. \qquad (23)$$

Consider an angular distribution of scattered neutrons. The polar axis is directed along the wave vector $\mathbf{k}_0$ of the incidence wave, and the axis x is in the plane of vectors $(\mathbf{k}_0, \mathbf{l})$ perpendicular to $\mathbf{k}_0$, where $\mathbf{l}$ is a unit vector along the rod axis. Then $\mathbf{k}_0\mathbf{l} = k \cos \theta_0$ and

$$\mathbf{q}\mathbf{l} = k \left(\cos \theta_0 - \cos \theta \cos \theta_0 - \sin \theta \sin \theta_0 \cos \varphi \right), \qquad (24)$$

where θ и φ are the angles of the vector $\mathbf{k}$ of the scattered wave. Equation (23) can be integrated over the azimuth angle φ; taking into account the symmetry of Eq. (24), we get

$$\frac{d}{d \cos(\theta)} \sigma(\theta, \theta_0) = u_0^2 a^2 \rho^4 \int_0^\pi 2 d\varphi \, \mathrm{sinc}^2 (q_l a) \left| \frac{J_1(q_\rho \rho)}{q_\rho \rho} \right|^2. \qquad (25)$$

After multiplication of the differential cross section (25) by a number of nanorods N_1 in the unit volume, we get the macroscopic differential cross section Σ:

$$\Sigma(\theta, \theta_0) = N_1 \frac{d}{d \cos(\theta)} \sigma(\theta, \theta_0) = A \int_0^\pi 2 d\varphi \, \mathrm{sinc}^2(q_l a) \left| \frac{J_1(q_\rho \rho)}{q_\rho \rho} \right|^2, \qquad (26)$$

where

$$A = \gamma \, u_0^2 \, a \rho^2 / 2\pi \qquad (26a)$$

and the value $\gamma = N_1 V_1 = N_1 2\pi \rho^2$ characterizes a fraction of volume occupied by nanorod matter. In the following, we will assume $\gamma = 0.1$. In order to describe precisely some concrete neutron nanorod reflectors, we will need a more accurate model. The dimension of the coefficient A is 1/cm, and its value depends on nanorod parameters. In order to compare neutron cross sections for different nanorods, we introduce a convenient common dimensional coefficient

$$A_0 = \frac{\gamma u_0^2 \rho_0^3}{2\pi}. \qquad (27)$$

6

If the nanorod radius is $\rho_0 = 10$ nm, then $A_0 = 3.4\ \mu m^{-1}$ (for diamond $1/\sqrt{u_0} \approx$ 8.27 nm). The macroscopic cross section of neutron scattering (26) can be presented in the following form:

$$\Sigma(\theta, \theta_0) = A_0 \frac{\bar{\rho}^3}{\beta} \int_0^\pi 2d\varphi \operatorname{sinc}^2(\bar{q}_l \alpha) \left| \frac{J_1(\bar{q}_\rho \alpha \beta)}{\bar{q}_\rho \alpha \beta} \right|^2, \qquad (28)$$

with dimentionless parameters $\bar{q} = q/k$, $\alpha = ak$, $\beta = \rho/a$, $\bar{\rho} = \rho/\rho_0$. The macroscopic differential cross section $\Sigma(\theta, \theta_0)$ of scattering of a neutron on powder of nanorods, in units $2A = 2A_0\bar{\rho}^3/\beta$, is shown in Fig. 1 ($a = 1000$ nm) and in Fig. 2 ($a = 10$ nm) as a function of the neutron scattering angle θ provided the neutron incidence angle θ_0 equals 0, $\pi/4$ and $\pi/2$, the nanorod radius $\rho = \rho_0 = 10$ nm, for two values of the nanorod half-length a, and for the neutron velocity $v = 450$ m/s. Angles are given in radians. Cross sections of neutron scattering on nanorods with the half-length equals radius $a = \rho$ are approximately equal to the cross section of neutron scattering on spherical nanoparticles of equal radius, therefore, in the following, we will use for simplicity the same analytical expressions for qualitative comparison of results for long nanorods and for spherical nanoparticles.

The average angle of neutron scattering on nanoparticles is equal approximately to the ratio of neutron wavelength to nanoparticle size. Thus, neutrons scatter on long nanorods to smaller angles (Fig. 1), than they scatter on short nanorods (Fig. 2). And the cross sections of neutron scattering to the zero angles are equal to each other as well as to $\pi/2$. The total scattering cross section is
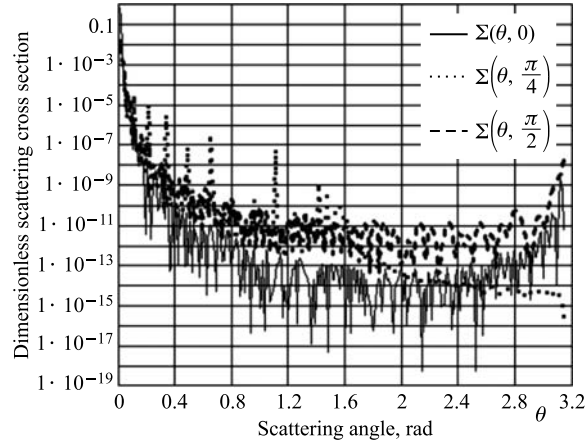
Fig. 1. Dimensionless differential cross section $\Sigma(\theta, \theta_0)$ of neutron scattering on a nanorod as a function of the neutron scattering angle θ and the neutron incidence angle θ_0. The angles are measured relative to the nanorod axis, $v = 450$ m/s, $a = 100\rho = 1000$ nm

7
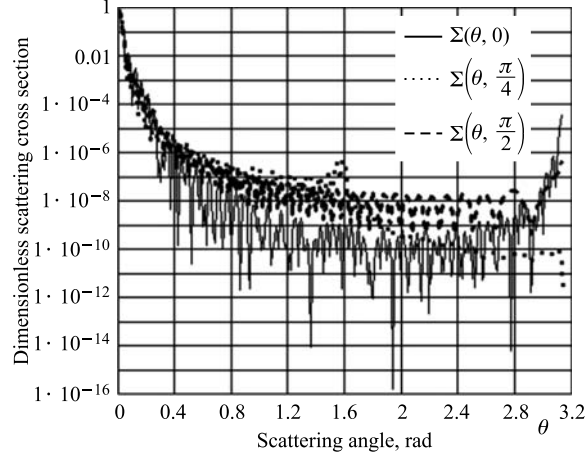
Fig. 2. The same as in Fig. 1, but for the nanorod half-length of $a = \rho = 10$ nm

smaller for larger neutron velocity. This peculiarity of neutron cross sections essentially explains a sharp decrease in efficiency of nanoparticle reflectors, while the neutron velocity increases from $v = 50$ m/s to $v = 450$ m/s. It is interesting to note some increase of cross sections for backscattering, which is particularly visible for nanorods.

Taking into account a factor $1/\beta$ in Eq. (28), we see that the cross section of small-angle neutron scattering on nanorods is much larger than that on nanospheres of equal diameter. As long nanorods, in contrast to nanospheres, provide an anisotropy axis (see Fig. 1 and Fig. 2), it is useful to consider separately the cases of chaotic and ordered orientation of long nanorods in reflectors.

In Sect. 4, we consider the reflection of isotropic VCN flux from a reflector built of chaotically oriented nanorods; in Sect. 6, we analyze the reflection of CN from a reflector built of nanorods with the axis parallel to the reflector surface while they are isotropically oriented over the azimuth angle.

4. CROSS SECTION OF NEUTRON SCATTERING ON CHAOTICALLY ORIENTED NANORODS

Averaging over directions $\boldsymbol{l}$ and multiplication by N_1 transform Eq. (23) into

$$d\Sigma_s(q, a, \rho)/d\Omega = A_0 \frac{\bar{\rho}^3}{\beta} \int_0^1 d\cos\vartheta \, \mathrm{sinc}^2(\cos\vartheta\bar{q}\alpha) \left| \frac{J_1(\sin\vartheta\bar{q}\alpha\beta)}{\sin\vartheta\bar{q}\alpha\beta} \right|^2 =$$

$$= A_0 \frac{\bar{\rho}^3}{\beta} \int_0^1 dx \, \mathrm{sinc}^2(x\bar{q}\alpha) \left| J_1\left(\sqrt{1-x^2}\bar{q}\alpha\beta\right) / \sqrt{1-x^2}\bar{q}\alpha\beta \right|^2. \quad (29)$$

8

In order to calculate the neutron albedo from powder of nanorods, we should know the cross section of backward scattering relative to the normal to the powder surface. We define the normal to surface to be the polar axis directed towards matter. Then the transferred momentum for backward scattered neutrons is

$$\bar{q}_b = \sqrt{2\left(1 + \cos\theta_0 \cos\theta - \sin\theta_0 \sin\theta \cos\varphi\right)}, \qquad (30)$$

where θ and φ are the scattered neutron angles, and axis x is in the incidence plane. We denote $y = \cos\theta_0 \cos\theta - \sin\theta_0 \sin\theta \cos\varphi$, integrate over $d\Omega = d\varphi d\cos\theta$, average over directions θ_0 of incidence neutrons, and present this expression, divided by $A_0 \bar{\rho}^3/\beta$, in the form

$$\Sigma_b(\alpha, \beta, \rho) = \int_{-1}^{1} dy \delta\left(y - \cos\theta_0 \cos\theta + \sin\theta_0 \sin\theta \cos\varphi\right)$$

$$d\Omega d\cos\theta_0 S(y, \alpha, \beta, \rho), \quad (31)$$

where

$$S(y, \alpha, \beta, \rho) = \int_0^1 dx \operatorname{sinc}^2(x\sqrt{2(1+y)}\alpha) \frac{J_1\left(\sqrt{1-x^2}\sqrt{2(1+y)}\alpha\beta\right)^2}{\sqrt{1-x^2}\sqrt{2(1+y)}\alpha\beta}, \quad (32)$$

and x denotes cosine of the nanorod axis relative to the transferred momentum q.

After integration of Eq. (31) over $d\varphi$, we get

$$\Sigma_b(\alpha, \beta, \rho) = \int_{-1}^{1} dy I(y) S(y, \alpha, \beta, \rho), \qquad (33)$$

where

$$I(y) = \int_0^1 d\cos\theta_0 \int_0^1 d\cos\theta \frac{\Theta\left(\sin\theta_0^2 \sin\theta^2 > (\cos\theta_0 \cos\theta - y)^2\right)}{\sqrt{\sin\theta_0^2 \sin\theta^2 - (\cos\theta_0 \cos\theta - y)^2}}, \quad (34)$$

and Θ is the step function, which is equal to 1 provided inequality in its argument, and is equal zero otherwise. Function $I(y)$ is calculated in (A4). It is equal to

$$I(y) = \pi\Theta(y > 0) - \operatorname{arctg}\left(\frac{\sqrt{1-y^2}}{y}\right). \qquad (35)$$

Figure 3 shows the dimensionless (in units A_0) macroscopic cross section $\Sigma bl(v) = \Sigma_b(15.8v, 0.01, 1)/\beta$ of neutron scattering as a function of its velocity v for powder of nanorods with the half-length $a = 1000$ nm, and the dimensionless macroscopic cross section $\Sigma bs(v) = \tilde{\Sigma}_b(0.158v, 1, 1)/\beta$ for powder of nanorods with the half-length of $a = 10$ nm.

9

The cross section $\Sigma b(v)$ shows minimum for the velocity of $v = 390$ m/s as the derivative of function $|J_1(x)/x|^2$ over x in the vicinity of $x \approx 20\pi$ oscillates rapidly around zero, and therefore integrals (32) and (33) tend this derivative to zero; this behavior explains minimum in the cross section of backward scattering
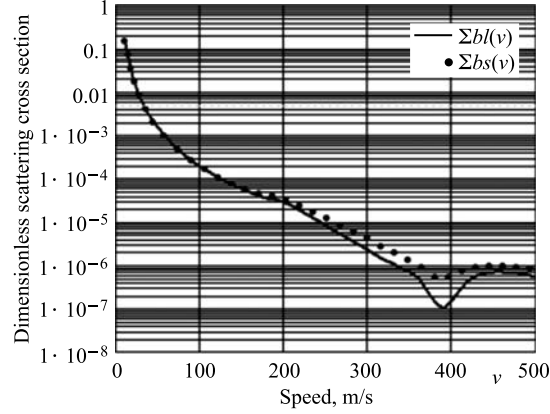
Fig. 3. Dimensionless macroscopic cross section of neutron backward scattering $\Sigma_b(v)$ (33) on powder of long nanorods ($\Sigma bl(v)$) with the half-length of $a = 1000$ nm and on powder of short nanorods ($\Sigma bs(v)$) with the half-length of $a = 10$ nm. In both cases, the nanorod radius equals $\rho = 10$ nm. Note that in spite of the term $1/\beta$, cross sections are equal at small velocities
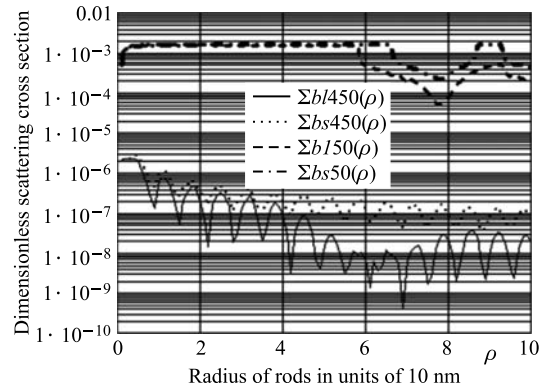
Fig. 4. Macroscopic cross section $\Sigma_b(\rho)$ of neutron scattering on powder of long nanorods with the half-length of $a = 100\rho$ nm for the neutron velocity of 450 m/s ($\Sigma bl450\,(\rho)$), on powder of short nanorods with the half-length $a = \rho$ nm for the neutron velocity of 450 m/s ($\Sigma bs450(\rho)$), on powder of long nanorods with the half-length $a = 100\rho$ nm for the neutron velocity of 50 m/s ($\Sigma bl50(\rho)$), and on powder of short nanorods with the half-length $a = \rho$ nm for the neutron velocity of 50 m/s ($\Sigma bs50(\rho)$)

10

in this point. This feature is apparently characteristic only for powder of nanorods with the ideal cylindrical shape.

Figure 4 shows dimensionless macroscopic cross section of neutron scattering $\Sigma bl450(\rho) = \Sigma_b(15.8 \cdot 450\rho, 0.01, \rho)\rho^3/\beta$ on powder of nanorods as a function of their radius ρ, in units 10 nm, for nanorods with the half-length $a = 100\ \rho$ for the neutron velocity of $v = 450$ m/s, and for nanorods with the half-length $a = \rho$: $\Sigma bs450(\rho) = \Sigma_b(0.158 \cdot 450\rho, 1, \rho)$, as well as analogous dependences for the velocity of 50 m/s.

5. ABSORPTION CROSS SECTION

The total cross section is defined by the imaginary part of the forward scattering amplitude (1)

$$\mathrm{Im}\,(F(\mathbf{q}, \mathbf{l}))_{q=0} = u_0'' a\rho^2/2 = N_0 k\sigma_1(k)\,a\rho^2/2 \qquad (36)$$

and it actually describes absorption as scattering in the perturbation theory is not included in this expression. The macroscopic cross section of absorption is equal:

$$\Sigma_a(k) = \frac{4\pi}{k} N_1 \mathrm{Im}\,(F(\mathbf{q}, \mathbf{l}))_{q=0} =$$
$$= \frac{4\pi}{k} N_1 \frac{1}{2} N_0 k\sigma_l(k)a\rho^2 = \frac{\gamma u_0^2 \rho_0^3}{2\pi} \frac{k_T \sigma_l(k_T)}{2kbu_0\rho_0^3} = A_0 \frac{C\bar{\rho}}{\alpha\beta}, \quad (37)$$

where $\bar{\rho} = \rho/\rho_0$ $\alpha = ka$, $\beta = \rho/a$ and

$$C = \frac{k_T \sigma(k_T)}{2u_0\rho_0^2 b} = \frac{\sigma(k_T)}{2bk_T(u_0/k_T^2)\rho_0^2}. \qquad (38)$$

T denotes the ambient temperature, $\rho_0 = 10$ nm, $b = 6.65$ fm, and $u_0/k_T^2 = E_c/E_T = 12 \cdot 10^{-6}$.

In the following, we will consider two cases of particular interest:

1. Nanoparticles at so small temperature that neutron heating in powder can be neglected, and also neutron cooling would even increase albedo. Also hydrogen in powder is substituted by deuterium, and neutron absorption in deuterium can be neglected. It is the case of most efficient reflector, which could be built using the principle considered in the present article. In this case, absorption cross section is attributed to one carbon atom; it is equal $\sigma_l(k_T) = 0.0035$ bn, and $C = C_0 = 6.28 \cdot 10^{-7}$.

2. Nanoparticles at the ambient temperature, with a realistic admixture of hydrogen. As nanopowder reflectors are most efficient for small neutron energy compared to the ambient temperature (energy), then inelastic neutron scattering

is equivalent to neutron loss. And inelastic scattering is governed by a relatively small admixture of hydrogen in powder. As shown in work [28], the minimum admixture of hydrogen atoms, which can be achieved by means of heating and degassing of powder, corresponds to the following composition $C_{12.4\pm0.2}H$, and the cross section of neutron scattering on the atom of residual hydrogen at the ambient temperature, measured for neutrons with the wavelength of 4.4 Å, equals 108 ± 2 bn. In this case, the efficient cross section per one atom of the composition is $\sigma_l(k_T) = 3.56$ bn. Thus $C = C_a = 5.2 \cdot 10^{-4}$.

The neutron albedo from an infinitely thick layer of nanorods, which we will call below simply r, instead of R_∞, is equal (18) to [25–27]:

$$r(\alpha, \beta, \bar{\rho}, C) = \frac{\sqrt{\Sigma_a + 2\Sigma_b} - \sqrt{\Sigma_a}}{\sqrt{\Sigma_a + 2\Sigma_b} + \sqrt{\Sigma_a}} = \frac{\sqrt{1 + Q(\alpha, \beta, \bar{\rho}, C)} - 1}{\sqrt{1 + Q(\alpha, \beta, \bar{\rho}, C)} + 1} \quad (39)$$

where

$$Q(\alpha, \beta, \bar{\rho}, C) = \frac{2\Sigma_b}{\Sigma_a} = \frac{2}{C}\Sigma_b(\alpha, \beta)\frac{\alpha\beta}{\bar{\rho}}. \quad (40)$$

The calculations of neutron albedo from an infinitely thick layer of nanorods as a function of the velocity v of incidence neutrons for long ($a = 1000$ nm) and short ($a = 10$ nm) nanorods, show that neutron albedo from nanostructured powder for the neutron velocity of $v = 450$ m/s is significantly larger than the coefficient of neutron reflection $5 \cdot 10^{-9}$ from continuous matter.

Besides the reflection from infinite matter, albedo is characterized also by the exponential attenuation in matter $\exp(-x/L)$, i.e., by the attenuation length (8):

$$L^{-1} = 2\sqrt{\Sigma_a}\sqrt{\Sigma_a + 2\Sigma_b} =$$
$$= 2\Sigma_a\sqrt{1 + Q(\alpha, \beta, \bar{\rho}, C)} = L_0^{-1}(C)\kappa^{-1}(\alpha, \beta, \bar{\rho}, C); \quad (41)$$

after substituting (37), we get

$$L_0(C) = \frac{1}{2CA_0}, \quad \kappa(\alpha, \beta, \bar{\rho}, C) = \frac{\alpha\beta}{\bar{\rho}\sqrt{1 + Q(\alpha, \beta, \bar{\rho}, C)}}, \quad (42)$$

and $L_0(C_a) = 0.02$ cm. Figure 5 shows $\kappa(v)$ dependences for powders of long and short nanorods for the coefficients of neutron absorption C_0 and C_a, which are denoted respectively $\kappa l0(v)$, $\kappa s0(v)$, $\kappa la(v)$ and $\kappa sa(v)$.

Consider now the neutron reflection from a layer of nanopowder with a finite thickness D. Albedo from such a layer is defined by the formula

$$R(D, \alpha, \beta, \bar{\rho}, C) = r(\alpha, \beta, \bar{\rho}, C) \times$$
$$\times \frac{1 - \exp(-2D/L(\alpha, \beta, \bar{\rho}, C))}{1 - r^2(\alpha, \beta, \bar{\rho}, C)\exp(-2D/L(\alpha, \beta, \bar{\rho}, C))}. \quad (43)$$
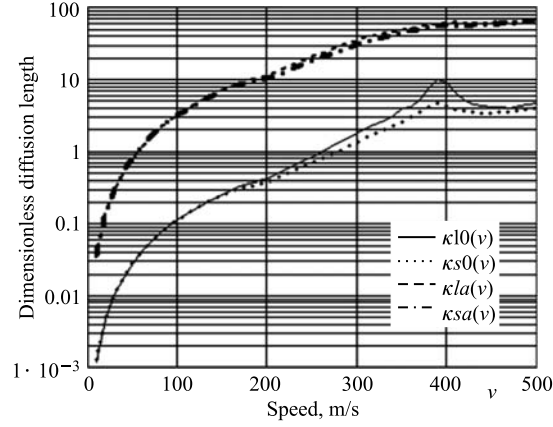
Fig. 5. Dimensionless diffusion length $\kappa(v) = L(v)/L_0(C)$ for long κl and short κs nanorods for the loss coefficients C_0 ($\kappa l0$ and $\kappa s0$) and C_a (κla and κsa)
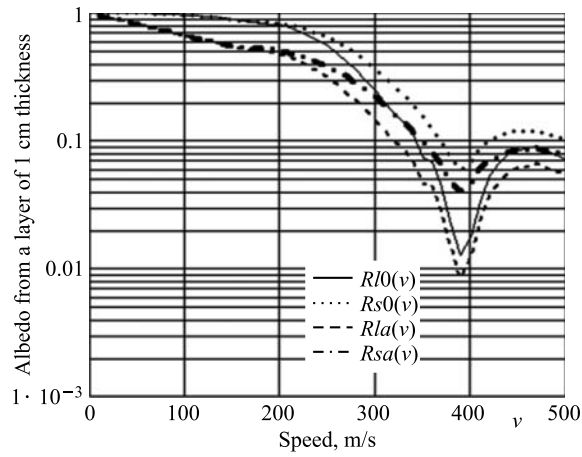
Fig. 6. Albedo $R(v)$ from powder of long, Rl, and short, Rs, nanorods with the thickness of $D = 1$ cm for the neutron loss coefficients C_0 ($Rl0$ and $Rs0$) and C_a (Rla and Rsa) as a function of neutron velocity

Figure 6 shows dependence $R(v)$ for the nanopowder thickness of $D = 1$ cm for long and short nanorods with the neutron loss coefficients C_0 and C_a, denoted respectively $Rl0(v)$, $Rs0(v)$, $Rla(v)$ and $Rsa(v)$. The figure shows that the neutron albedo from a sufficiently thin layer of nanoparticles is higher by 6–7 orders of magnitude than neutron reflection from continuous matter.

13

6. AXIS OF NANORODS IS ORIENTED PARALLEL TO THE INTERFACE

Now nanorods are parallel to the powder surface. We define the polar axis along the normal to the interface directed towards matter, and axis x is in the incidence plane. Then

$$\bar{q}_l = \bar{\mathbf{q}} \cdot \mathbf{l} = \sin\theta_0 \cos\chi - \sin\theta \cos(\varphi - \chi), \tag{44}$$

where χ is the azimuth angle of the nanorod orientation, and φ is azimuth scattering angle. Then

$$\bar{q}_\rho = \sqrt{2(1 + \cos\theta\cos\theta_0 - \sin\theta\sin\theta_0\cos\varphi) - }$$
$$\sqrt{-(\sin\theta_0\cos\chi - \sin\theta\cos(\varphi - \chi))^2}. \tag{45}$$

After averaging over nanorod orientation, integrating over backward scattering angles, and averaging over angular distribution of incident neutrons, we get

$$\Sigma_b(\alpha, \beta, \rho) = \int_0^1 du \int_0^1 dv \, \Sigma_{b\theta}(u, v, \alpha, \beta, \rho), \tag{46}$$

where

$$\Sigma_{b\theta}(u, v, \alpha, \beta, \rho) =$$
$$= \frac{\bar{\rho}^3}{\beta} \int_0^{2\pi} d\varphi \int_0^{2\pi} \frac{d\chi}{2\pi} \operatorname{sinc}^2(\alpha \bar{q}_l(u, v, \varphi, \chi)) \left| \frac{J_1(\bar{q}_\rho(u, v, \varphi, \chi)\alpha\beta)}{\bar{q}_\rho(u, v, \varphi, \chi)\alpha\beta} \right|^2. \tag{47}$$

Numerical integration of (47) gives an idea on the macroscopic cross section of neutron backward scattering $\Sigma_{b\theta}(\cos\theta, \cos\theta_0, \alpha, \beta, \rho)$ as a function of $u = \cos\theta$ for given values of $\nu = \cos\theta_0$. This dependence for long nanorods ($\beta = 0.01$) at $\bar{\rho} = 1$, the neutron velocity $v = 450$ m/s and two values of cosine of the incident angle $\cos\theta_0 = 0.3$ and 0.8 is shown in Fig. 7. One clearly sees in the figure the peaks in the vicinity of $\cos\theta = \cos\theta_0$, i.e., quasi-specular reflection is revealed.

Integration in (46) and substitution into albedo formulas allows one to get the results shown in Fig. 8. Here we show neutron albedo from a layer with the thickness of 3 cm as a function of the neutron speed v; the layer consists of long and short nanorods oriented along the interface but isotropically with respect to the azimuth around the interface normal. Albedo is calculated for small and large content of hydrogen. It is seen that albedo from long nanorods is higher than that from short ones, also that results of calculations are in agreement with the experimental observations for v in the range 50–150 m/s [10].

14
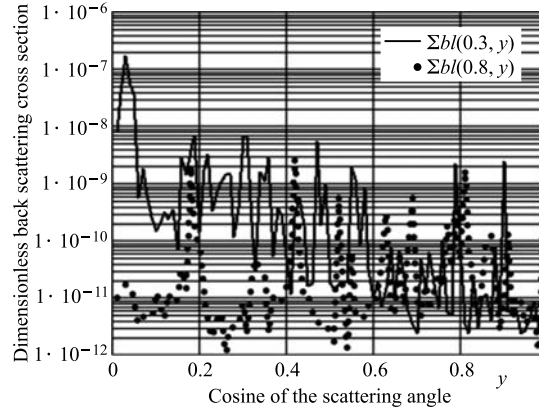
Fig. 7. Dependences Σ_b ($\cos \theta_0$, $\cos \theta$) from the neutron scattering angle θ and the neutron incidence angle θ_0 for long nanorods: $a = 1000$ nm and $\rho = 10$ nm for $v = 450$ m/s
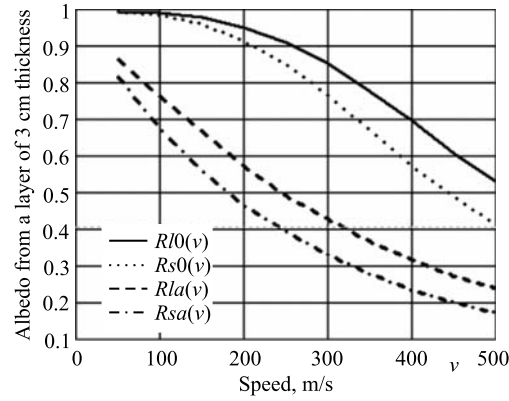
Fig. 8. Albedo $R(v)$ from powder of long ($a = 1000$ nm) and short ($a = 10$ nm) nanorods with the radius $\rho = 10$ nm with the layer thickness of $D = 3$ cm for two loss coefficients $C_0 = 6.28 \cdot 10^{-7}$ and $C_a = 5.2 \cdot 10^{-4}$ as a function of neutron velocity

7. A PROBLEM OF ACCOUNTING
FOR THE REAL ANGULAR DISTRIBUTION

We have assumed above that albedo is calculated for the isotropic distribution of reflected and incident neutrons. How would change the results, if one does not keep these assumptions? In order to answer this question, one has to solve

15

Eq. (13) in its general form. It is an extremely complex problem involving a nonlinear integral equation.

It can be simplified, provided a natural assumption that all functions depend only on cosines of incidence and reflected angles. Then the integral equation can be reduced, following discretization, to a matrix equation of the second order in the form $\hat{\mathbf{Z}}\hat{\mathbf{A}}\hat{\mathbf{Z}} + \hat{\mathbf{B}}\hat{\mathbf{Z}} + \hat{\mathbf{Z}}\hat{\mathbf{B}} + \hat{\mathbf{A}} = 0$. However solving such a quadratic matrix algebraic equation also is a complex problem. In fact, a quadratic matrix equation for the matrix $N \times N$ is equivalent in the general form to a polynomial equation with the power $2N^2$. And even if one calculates numerically all its roots, there will stay a problem of choosing a proper set of roots.

Nevertheless, one could try to consider an option, which will shed light on a role of anisotropy. For instance, one could search for a solution of Eq. (13) not in the purely isotropic form (14), but as a combination of isotropic and specular distributions in the form (48), where the specular part is presented by the diagonal term. This option will be considered in the following work:

$$\hat{\mathbf{R}} = R_\infty \int_{n\Omega<0} |\Omega\rangle \frac{|\cos\theta|}{\pi} d\Omega \int_{n\Omega>0} d\Omega' \langle\Omega'| + \int_{n\Omega<0} |\Omega\rangle f(\theta)\, d\Omega \langle\Omega|. \quad (48)$$

CONCLUSION

In the present theoretical work, we considered a possibility to increase efficiency of nanostructured reflectors of slow neutrons by means of substituting spherical nanoparticles by nanorods. We show that albedo of VCN from powder of disordered nanorods is smaller than their albedo from powder of nanospheres. However, albedo of VCN and quasi-specular reflection of CN from powder of nanorods oriented parallel to the reflector surface exceed respective values for powder of nanospheres.

APPENDIX

Denote $\cos\theta = v$, $\cos\theta_0 = u$. Then integral (34) is presented in the form

$$I(y) = \int_0^1 du \int_0^1 dv \frac{\Theta\left(1 - u^2 - v^2 > y^2 - 2yuv\right)}{\sqrt{1 - u^2 - v^2 - y^2 + 2yuv}} = \int_0^1 du\, I_1(u,y), \quad (A.1)$$

where integral $I_1(u, y)$, after variable substitution $x = (v - uy)/\sqrt{1 - u^2}\sqrt{1 - y^2}$ is deduced to the form

$$I_1(u, y) = \int\limits_{-x_1(u,y)}^{x_2(u,y)} dx \frac{\Theta\left(x^2 < 1\right)}{\sqrt{1 - x^2}} =$$

$$= \frac{\pi}{2} + \frac{\pi}{2}\Theta(u > \sqrt{1 - y^2})\frac{y}{|y|} + \arcsin\left(x_1(u, y)\right)\Theta(u < \sqrt{1 - y^2}). \quad (A.2)$$

Limits of integration in (A.2) are

$$x_1(u, y) = \frac{uy}{\sqrt{(1 - u^2)(1 - y^2)}}, \quad x_2(u, y) = \frac{1 - uy}{\sqrt{(1 - u^2)(1 - y^2)}}. \quad (A.3)$$

Modulus of these limits have to be smaller than unit, but $x_2(u, y) \geqslant 1$ for any values of u and y, therefore the upper limit, due to the inequality in the integral, has to be replaced by unit. The lower limit, $|x_1(u, y)| \geqslant 1$, if only $u \leqslant u_1(y) = \sqrt{1 - y^2}$; if $u > u_1(y) = \sqrt{1 - y^2}$, then modulus of the lower limit has to exceed unit and thus the lower limit should be replaced by -1 or $+1$ in function of a sign of y. Account for all these conditions results to (A.2). Substitution (A.2) into (A.1) and integration by parts of the term including arcsin provides the final result:

$$I(y) = \int\limits_0^1 du\, I_1(u, y) = \frac{\pi}{2}\left[1 + \left(1 - \sqrt{1 - y^2}\right)\frac{y}{|y|}\right] + \sqrt{1 - y^2}\frac{y}{|y|}\frac{\pi}{2} -$$

$$- \int\limits_0^{\sqrt{1-y^2}} \frac{uduy}{(1 - u^2)\sqrt{1 - u^2 - y^2}} = \pi\Theta(y > 0) - \operatorname{arctg}\left(\frac{\sqrt{1 - y^2}}{y}\right). \quad (A.4)$$

REFERENCES

1. *Luschikov V. I. et al.* Observation of ultracold neutrons // JETP Lett. 1969. V. 9. P. 23.
2. *Ignatovich V. K.* The Physics of Ultracold Neutrons. Oxford, UK: Clarendon Press, 1990.
3. *Golub R., Richardson D. J., Lamoreux S. K.* Ultracold Neutrons. Bristol: Higler, 1991.
4. *Mezei F.* Novel Polarized Neutron Devices — Supermirror and Spin Component Amplifier // Commun. Phys. 1976. V. 1. P. 81.
5. *Maruyama R. et al.* Development of Neutron Supermirrors with Large Critical Angle // Thin Solid Films. 2007. V. 515. P. 5704.

6. *Amaldy E., Fermi E.* On the Absorption and the Diffusion of Slow Neutrons // Phys. Rev. 1936. V. 50. P. 899.

7. *Nesvizhevsky V. V.* Interaction of Neutrons with Nanoparticles // Phys. At. Nucl. 2002. V. 65. P. 400.

8. *Artem'ev V. A.* Estimation of Neutron Reflection from Nanodispersed Materials // At. Energy. 2006. V. 101. P. 901.

9. *Nesvizhevsky V. V. et al.* The Reflection of Very Cold Neutrons from Diamond Powder Nanoparticles // Nucl. Instr. Meth. A. 2008. V. 595. P. 631.

10. *Lychagin E. V. et al.* Storage of Very Cold Neutrons in a Trap with Nanostructured Walls // Phys. Lett. B. 2009. V. 679. P. 186.

11. *Lychagin E. V. et al.* Coherent Scattering of Slow Neutrons at Nanoparticles in Particle Physics Experiments // Nucl. Instr. Meth. A. 2009. V. 611. P. 302.

12. *Nesvizhevsky V. V. et al.* Application of Diamond Nanoparticles in Low-Energy Neutron Physics // Materials. 2010. V. 3. P. 1768.

13. *Cubitt R. et al.* Quasi-Specular Reflection of Cold Neutrons from Nano-Dispersed Media at Above-Critical Angles // Nucl. Instr. Meth. A. 2010. V. 622. P. 182.

14. *Nesvizhevsky V. V.* Reflectors for VCN and Applications of VCN // Rev. Mexicana Fiz. 2011. V. 57. P. 1.

15. *Golub R., Pendlebury J. M.* Superthermal Sources of Ultracold Neutrons // Phys. Lett. A. 1975. V. 53. P. 133.

16. *Schmidt-Wellenburg Ph. et al.* Ultracold Neutron Infrastructure for the Gravitational Spectrometer GRANIT // Nucl. Instr. Meth. A. 2009. V. 611. P. 267.

17. *Baessler S. et al.* The GRANIT Spectrometer // Comp. Rend. Phys. 2011. V. 12. P. 707.

18. *Luschikov V. I., Frank A. I.* Quantum Effects Occuring When Ultracold Neutrons Are Stored on a Plane // JETP Lett. 1978. V. 28. P. 559.

19. *Nesvizhevsky V. V. et al.* Quantum States of Neutrons in the Earth's Gravitational Field // Nature. 2002. V. 415. P. 297.

20. *Irifune T. et al.* Materials — Ultrahard Polycrystalline Diamond from Graphite // Nature. 2003. V. 421. P. 599.

21. *Dubrovinskaia N. et al.* Aggregated Diamond Nanorods, the Densest and Least Compressible Form of Carbon // Appl. Phys. Lett. 2005. V. 87. P. 083106.

22. *de Carli P. S., Jamieson J. C.* Formation of Diamond by Explosive Shock // Science. 1961. V. 133. P. 1821.

23. *Aleksenskii A. E. et al.* The Structure of Diamond Nanoclusters // Phys. Solid State. 1999. V. 41. P. 668.

24. *Dolmatov V. Yu.* Detonation Nanodiamonds: Synthesis, Structure, Properties and Applications // Uspekhi Khimii. 2007. V. 76. P. 375.

25. *Ignatovich V. K., Shabalin E. P.* Algebraic Method for Calculating a Neutron Albedo // Phys. At. Nucl. 2007. V. 70. P. 265.

26. *Ignatovich V. K.* Neutron Optics. M.: Nauka, Fizmatlit, 2006 (in Russian).

27. *Utsuro M., Ignatovich V. K.* Handbook of Neutron Optics. Berlin: Wiley-VCH, 2010.

28. *Krylov A. R. et al.* Study of Bound Hydrogen in Powders of Diamond Nanoparticles // Crystallography Rep. 2011. V. 56. P. 102.

29. *Nesvizhevsky V. V. et al.* Neutron Whispering Gallery // Nature Phys. 2010. V. 6. P. 114.

30. *Nesvizhevsky V. V.* Near-Surface Quantum States of Neutrons in the Gravitational and Centrifugal Potentials // Physics-Uspekhi. 2010. V. 53. P. 645.

31. *Nesvizhevsky V. V.* Gravitational Quantum States of Neutrons and the New GRANIT Spectrometer // Mod. Phys. Lett. A. 2012. V. 27. P. 1230006.